Tribology of Tidal Turbine Blades: Impact angle effects on erosion of polymeric coatings in sea water conditions

Ghulam Rasool, Cameron Johnstone and Margaret M. Stack

Department of Mechanical & Aerospace Engineering, University of Strathclyde

Glasgow, UK
Ghulam.rasool@strath.ac.uk
Cameron.Johnstone@strath.ac.uk
Margaret.Stack@strath.ac.uk

Abstract

Tidal energy, of all marine renewables energies, possesses higher persistency and predictability over long time scales. Due to the aggressive marine environment, there are barriers in the development of tidal power generation technology. In particular, with regard to increased rotor diameter, the selection of material presents significant challenges to be addressed including the tribological environment, such as solid particle erosion, cavitation erosion, the effect of high thrust loading on the turbine blade tips, and the synergy between sea water conditions and such tribological phenomena. This research focuses on producing and testing a variety of advanced materials and surface coatings to investigate two main tribological issues in tidal environments: matrix cutting and reinforcement fracture. In our previous work, a G10 epoxy glass laminate was tested in this environment and the results revealed tribological issues. In this present work, G10 epoxy glass laminate base erosion resistant polymeric coatings have been tested for the range of sand particles size in our our previous work and in NaCl solution. The test results reveal that the coating has enhanced the quality of performance of the composite with respect to tribological behaviour, and has diminished the synergy between sea water and tribological phenomena. This indicates progress toward the selection of advanced materials to manufacture tidal turbine blades.

1. Introduction

New and renewable energy sources and related technologies are essential components of the path towards sustainable development. Although renewable sources represent the fastest growing energy source in the world, they still have to overcome many technical and financial barriers to achieve their full potential in the market [1]. Globally, 330,000 terawatt hours electricity per year can be produced from offshore energy resources [2]. Despite different technical and financial challenges, tidal turbines have been forefront in the introduction of marine renewable energy technologies due to the well documented behaviour of the tides and reliable power delivery on every tide. Moreover, the higher density of seawater and contra rotating blade configuration are other advantages in generation of greater power output from a tidal turbine compared with a wind turbine of

similar dimensions in comparable fluid flow velocities [3]. The net effect on the tidal turbine blade structure is higher forces within a smaller envelope, which requires maximum possible performance from the materials used to manufacture the blades.

For the growth of tidal energy, there are still technical challenges and financial barriers to overcome. There is still no agreement on the optimum design, and materials selection especially for tidal turbine blade. Hence, the use of more reliable, cheaper and advanced material, and surface treatment techniques can contribute in cost reduction of electric power generation by this source.Likewise as for wind turbine blades, fibre reinforced composite materials can be used to manufacture tidal turbine blades as they possess good mechanical properties; corrosion resistance, and generally cost effectiveness. However, due to the aggressive marine environment, identifying a reliable composite material, especially with an increased turbine rotor diameter, raises further tribological issues to be addressed, such as sediment and solid particle erosion, cavitation erosion and their possible synergistic effects on the tidal turbine blades [4]. In our previous work, a G10 epoxy glass laminate was tested in various solution sand slurries, which presented some tribological related materials issues, [5]. These issues were weight gain, interaction of salt solution with the resin, de-bonding at fibre-matrix interface and exposure of reinforcement fibres, cutting of the matrix, pit formations, cracks, blistering of the laminate, swelling of matrix, fibre fracture, platelet and flake formation etc.

To overcome these tribological challenges, a protective barrier layer, between the seawater and composite, in the shape of a polymeric surface coating was used to enhance the quality of performance and the life span of such materials. The polymeric compositions are rapid and cold-curing surface coatings processes which can be carried out either by hand brush or by spraying method. By replicating marine conditions, tests were carried out on slurry pot test rig to measures the effects of different impact angles and particles sizes at constant tip speeds. Tests have revealed that the erosion resistant polymeric coating has enhanced the quality of performance with respect to tribological aspect along with resistant to mass gain.

In this paper, the erosive wear behaviour of composite (uncoated and coated with erosion resistant polymeric coatings) in seawater conditions has been studied. The tribological investigations have been carried out on the basis of mass gain, volume loss, SEM micrographs of the worn surfaces, EDX analysis, and related research work found in the literature. This is a significant progress toward selection of composite materials for use as tidal turbine blades. Further work will involve assessing the performance of different coatings such as polymeric, gel, silicone, rubber or composition of these materials.

2. Experimental

2.1. Material

A G10 epoxy glass laminate composite, manufactured by National Electrical Manufacture Association (NEMA) was used as uncoated specimen and substrate for application of erosion resistant polymeric coatings. This material is widely used in electrical equipment of aerospace, medical diagnostic and underwater conditions. It is also used for mechanical applications when outstanding strength, stiffness, and excellent creep resistance are required. This thermosetting industrial composite consists of continuous filament glass cloth and epoxy as the resin binder. The sizes of the specimen were 60 mm in length, 25 mm in breadth and 6 mm in thickness. The general characteristic of this material is the high strength, low moisture absorption and excellent chemical resistance in dry and humid conditions. The mechanical and physical properties of this material are listed in Table 1.

G10 epoxy glass laminate	
Flexural strength (MPa)	482
Tensile strength (MPa)	320
Shear strength (MPa)	131
Impact (Notched CHARPY) (kJ m^{-2})	65
Density (g cm^{-3})	2
Specific gravity	1.82
Water absorption (mg m^{-2})	8
Hardness, Rockwell (M-scale)	110
Standard finish	Satin/Glossy
Body colour	Green

Table 1 – Physical properties of the G10 epoxy glass laminate

Figure 1 COMPO (a) shows the SEM micrograph of the G10 epoxy glass laminate uncoated surface before the test. The faded brighter areas can be trapped micro-bubbles under the glossy surface or the residual dust during finishing the side surfaces of the rectangular specimens.

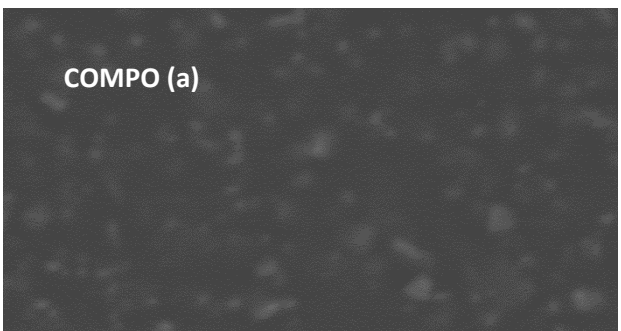

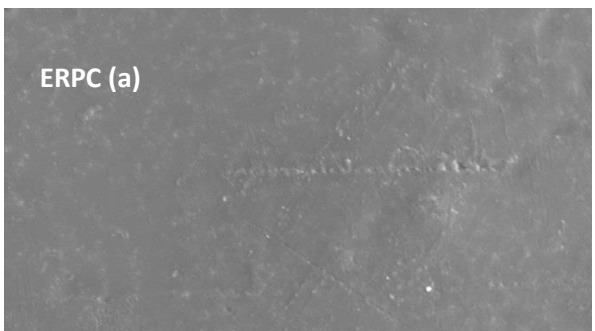

Fig. 1 – SEM micrograph composite, (a) uncoated surface and, (b) coated surface

2.2. Coating

Belzona Product: 1331 was used as erosion resistant polymeric coating material.

2.2.1. Substrate surface preparation and coating process

To ensure an effective adhesion (mechanical bond created by the surface preparation process), the composite specimens surfaces were blasted to 3mils (75 microns) with chilled iron grit of average size 100 microns. Loose particles were brushed away and degrease with a rag soaked in Belzona 9111 cleaner/degreaser. After blasting and cleaning, specimen surfaces can be coated with hand brush or spraying method. In this case, specimens were coated by hand with a short bristled brush, (it was too impractical to spray due small size of the specimen). The two coats of 1331 were applied @ 250 microns each for maximum average thickness of 500microns. Figure 1 ERPC (a) shows the SEM micrograph of the G10 epoxy glass laminate base polymeric coatings surface before the test. The mechanical and physical properties of 1331 Polymeric erosion resistant coatings are listed in Table 2.

Polymeric erosion resistant coating	
Flexural strength (MPa)	43.1
Tensile shear strength (MPa)	26.9
Compressive yiel strength (MPa)	39.8
Shear strength (MPa)	26.9
Pull off adhesion (Posi Test Dolly Pull Off) (MPa)	22.1
Density (g cm^{-3})	1.14
Water absorption (mg m^{-2})	Nil
Hardness, Shore D	77
Standard finish	Glossy

Body colour	White

Table 2 – Mechanical and physical properties of the polymeric erosion resistant coatings

2.3. Test Slurry

The tests were conducted in NaCl solution and NaCl solution + Sand particles size (200 ± 50 µm), Sand I, and Sand particle size (425 ± 175 µm), Sand II. The sand was supplied by Mineral Marketing. The sand particles were sieved twice in the lab to ensure the size of the particles. The specific gravity sand was 2.65, and bulk density of the particles was 1.56 g cm^{-3}. It should be noted that the concentration of the silica sand defines the density of the slurry. Higher concentration provides higher density and requires more energy for the suspension. Moreover, higher concentration also causes the distribution of the particles to become uneven [6]. Therefore, a concentration similar to the seabed environment was maintained during the all tests. The chemical composition of the silica sand used is mentioned in Table 3.

Chemical composition of the silica sand (%)

SiO_2	Fe_2O_3	Al_2O_3	K_2O	CaO	Na_2O	LOI
99.72	0.048	0.07	0.02	<0.01	0.04	0.05

Table 3 – Chemical composition of the sand particles

2.4. Testing Apparatus

Experimental work was carried out in a slurry pot test rig. The rig consists of a test chamber and two motors one at the top and the other at the bottom of the test chamber Fig. 2(a). The upper motor functioned as a miniature tidal turbine rotor with blade inserts and the bottom motor worked as a stirrer of slurry. In Figure 2(b), the test chamber showing the sample holder inserted test specimens, and the direction of the slurry movement are indicated. The sample holder, which acted as a hub of the turbine rotor, has different angled slots to insert the specimens. The angle of attack range was 0 – 90^o with 15^o increment. The four baffle bars are installed in the test chamber. The role of these baffles is to prevent unwanted swirling of the flow due to the rotation of the samples, to maintain axial flow and to minimise centrifuging effect of the fluid inside the test chamber. Both motors rotate in opposite directions to avoid random motion of the particles, turbulence of the flow and error in the calculation of the impingement velocity. The four blades of the bottom motor (stirrer) are pitched at 45^o, which is the optimal degree to provide a better particles distribution and down-pumping of solutions to give axial flow in the test chamber as shown in figure 2(b), [6 - 9].

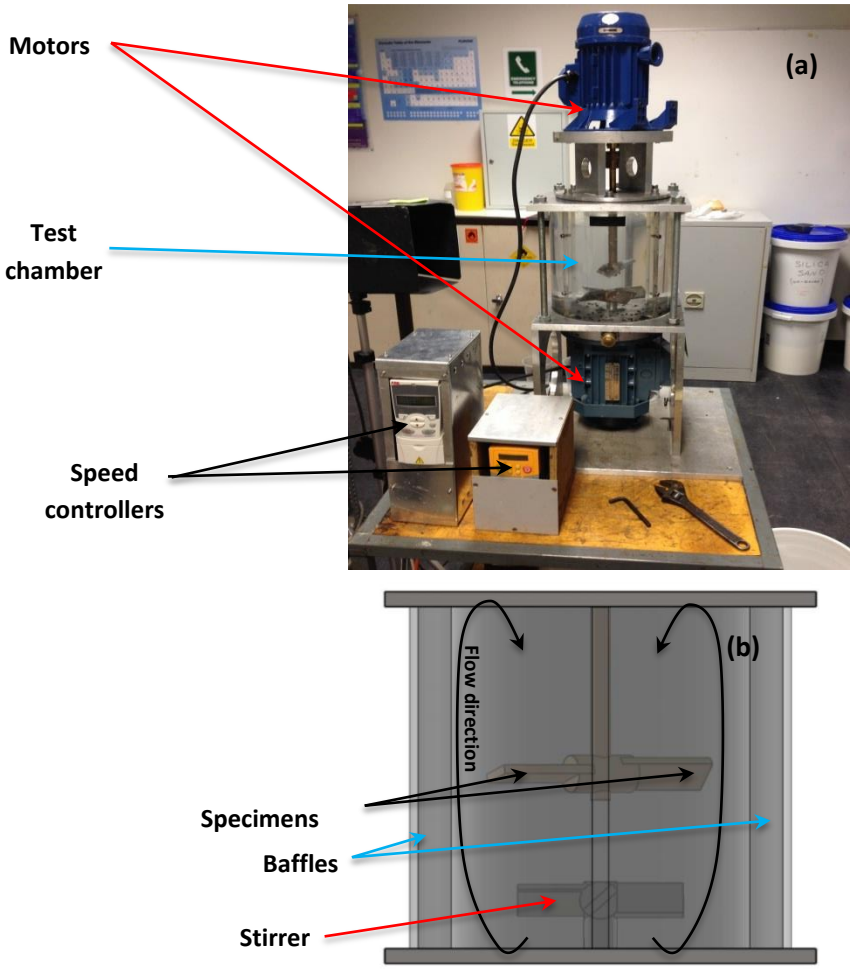

Figure 2 – (a) Slurry pot testing rig and (b) Test chamber

2.5. Test Conditions and Parameters

a. Test temperature: Tests were carried out at room ambient conditions.

b. Impingement angles: 0^{o}, 15^{o}, 30^{o}, 45^{o}, 60^{o}, 75^{o}, and 90^{o}.

c. NaCl solution, and NaCl solution and sand slurry.

d. Salinity (wt. %): 3.5.

e. Sand concentration (wt. %): 3.

f. Test duration: 2 hrs.

g. Sand particles size (µm): (200 ± 50), Sand I, and (425 ± 175), Sand II.

h. Sand particles shape: washed and graded sand of sub angular to rounded grain.

i. Linear tip speed (m s^{-1}): 3.

2.6. Erosion Tests

In order to measure the effects of the angles of attack on marine tidal turbine blades, the samples were tested at seven different angles. The samples were weighed before and after the tests carried out by using an analytical balance with an accuracy of 0.01 mg to the nearest 0.0001g. The orientation of the angles of the test specimens was considered as the angles of impingement of the solid particles [7]. As recommended by Tsai et al., to avoid the presence of vortices, which can affect the test results from a slurry pot tester, a lower rotational speed of the specimens was employed [9]. This was empirically tested by using a high speed camera and large polymer particles by observing the trajectory of the particles to confirm that they were following the flow direction of the solution. At a tip speed, 3 m s^{-1}, the flow of solution was completely in axial direction as shown in Fig. 2(b). This tip speed was optimised with respect to frequencies of the motor for all the combinations of slurry and angle of attack and maintained during the tests.

In this type of test configuration, uniform distribution of the sand particles is very important which is controlled by the speed of the stirrer (bottom motor). Although it may be thought that the higher speed of the stirrer can provide a better suspension, but this can cause a turbulent flow and appearance of vortices [8]. Therefore, the speed of the stirrer was optimised as well for the full suspension of the particles and maintained during the tests. The optimised speed of the stirrer was 309 rpm which was equal to 11 Hz and 22% of the bottom motor output. The test chamber was completely immersed with the solutions to eliminate the appearance of bubbles from the residual air in the chamber and avoid their disturbance. The NaCl solutions + sand slurry were replaced every half an hour to minimise the attrition of the sand particles. The attrition of the sand particles after half an hour test run was found to be 2.59 wt. % on average.

The duration of each test 2 hours was chosen in accordance with the tests reported in the literature in order to keep the comparability of the results. After completing each test, the samples were washed with normal water and dried by keeping under a gentle heat for 15 minutes and held at room temperature. The mass loss measurements of the tested samples were carried out on the next day of the tests to minimise the errors from the solution absorbability. Then the mass losses were converted to volumes losses, for comparison, as the composite and polymeric coatings had different densities. The exposed surfaces of the specimens were examined by scanning electron microscopy (SEM) together with EDX analysis to investigate the erosion mechanisms.

3. Tests Results and Discussion

3.1. In NaCl Solution

3.1.1. Mass Gain

Figure 3 shows the erosion test results of the composite, uncoated and coated with polymeric coatings, in NaCl solution only. The uncoated specimens have gained mass at

each angle of attack. Despite G10 epoxy glass laminate being recognised for its low porosity and good adhesion between its components, the NaCl solution enters into the polymeric matrix composite by a diffusion process through pores in the matrix, result in an increase in the mass after the tests carried out. The polymeric coating not only acts as a barrier between substrate and NaCl solution but also does not absorb any solution to gain its mass, Fig. 3(a). The polymeric coatings can be used to slow the ingress of the moisture in composite materials. The effectiveness of these coatings is limited by the quality and thickness as well moisture diffusivity and solubility [10]. It is evident from these results that the coating has negated the mass gain and interaction of the NaCl solution with substrate. Figure 3(b) shows the total mass gained by the uncoated and coated samples for the range of angle of attack in NaCl solution. The total mass gained by the composite is very prominent in comparison with coating. Mass gain is an important factor that characterise the performance change of material in the whole degradation process [11-13].

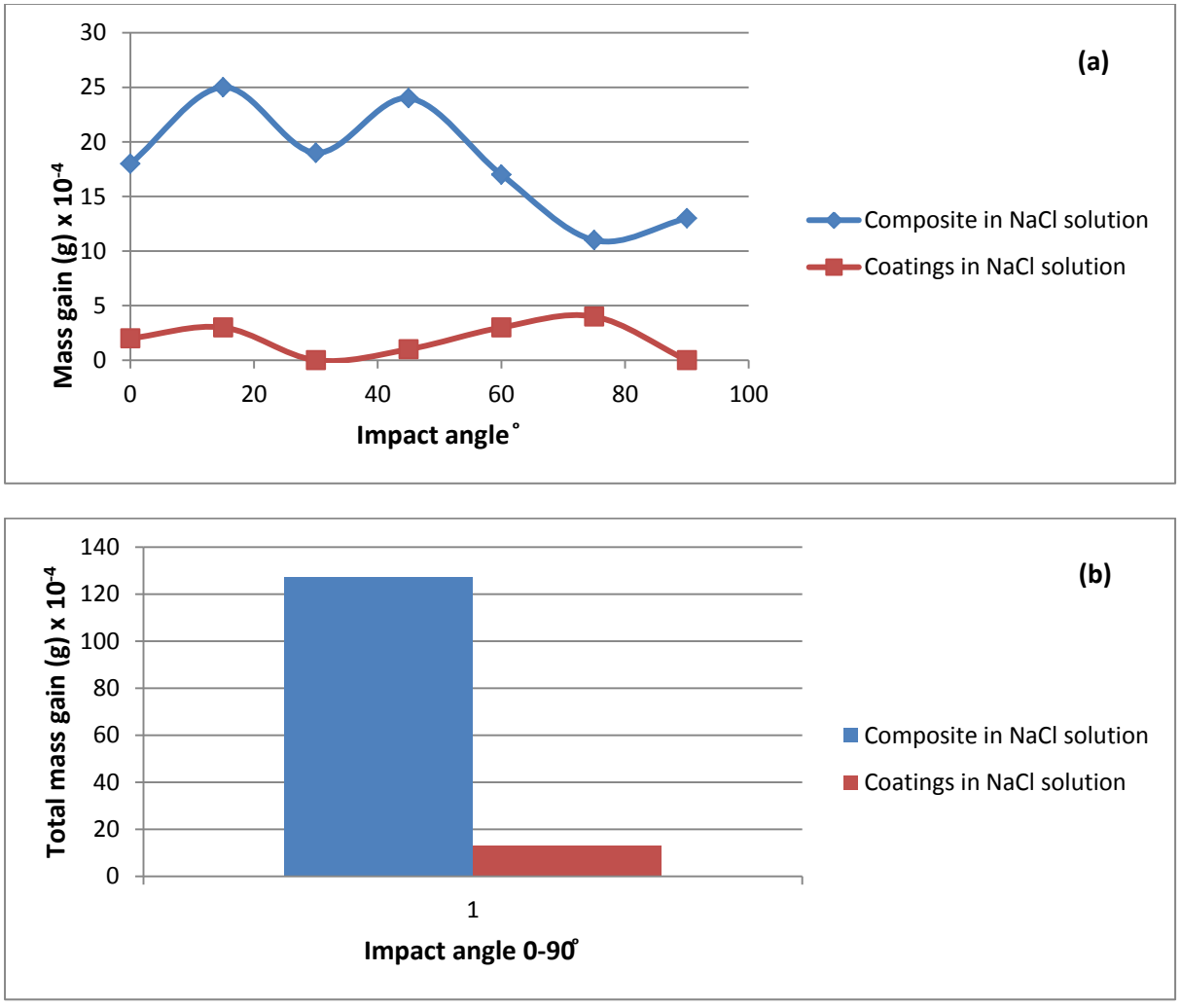

Figure 3– Mass gain of composite and coatings specimens as a function of impact angle in NaCl solution (a) at various impact angles (b) total mass gain in NaCl solution.

3.1.2. SEM micrographs and EDX analysis of the uncoated composite specimen exposed surface in NaCl solution at 60° angle of attack.

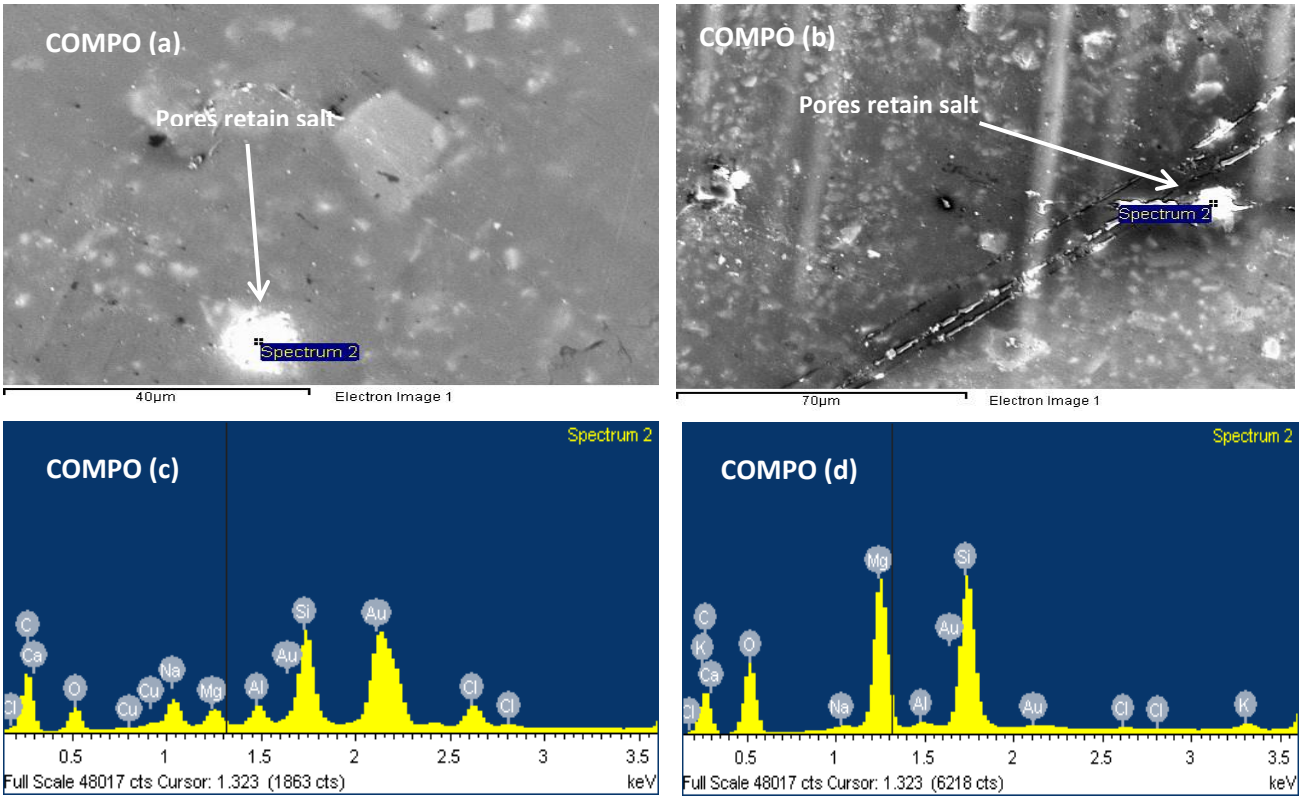

Fig. 4 – Composite exposed surface SEM and EDX after a test in NaCl solution at 60° angle of attack (a) site 1, (b) site 2, (c) EDX analysis of (a), and (d) EDX analysis of (b).

3.1.3. SEM micrographs and EDX analysis of the composite base erosion resistant polymeric coatings exposed surface in NaCl solution at 60° angle of attack.

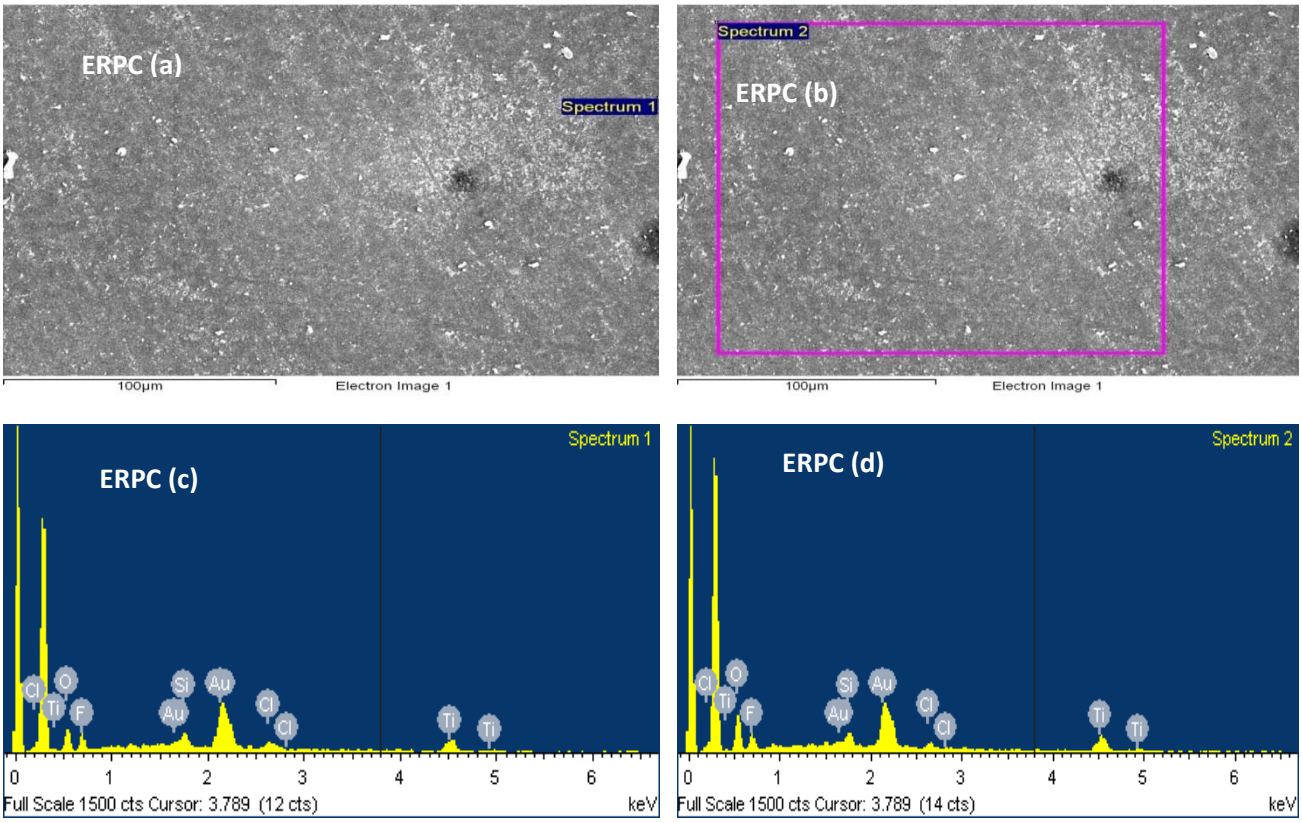

Fig. 5 – Erosion resistant polymeric coatings exposed surface after a test in NaCl solution at 60^{o} angle of attack (a) site 1, (b) site 2, (c) EDX analysis of (a), and (d) EDX analysis of (b).

3.1.4. SEM micrographs of the uncoated and coated exposed surfaces in NaCl solution at 60^{o} angle of attack.

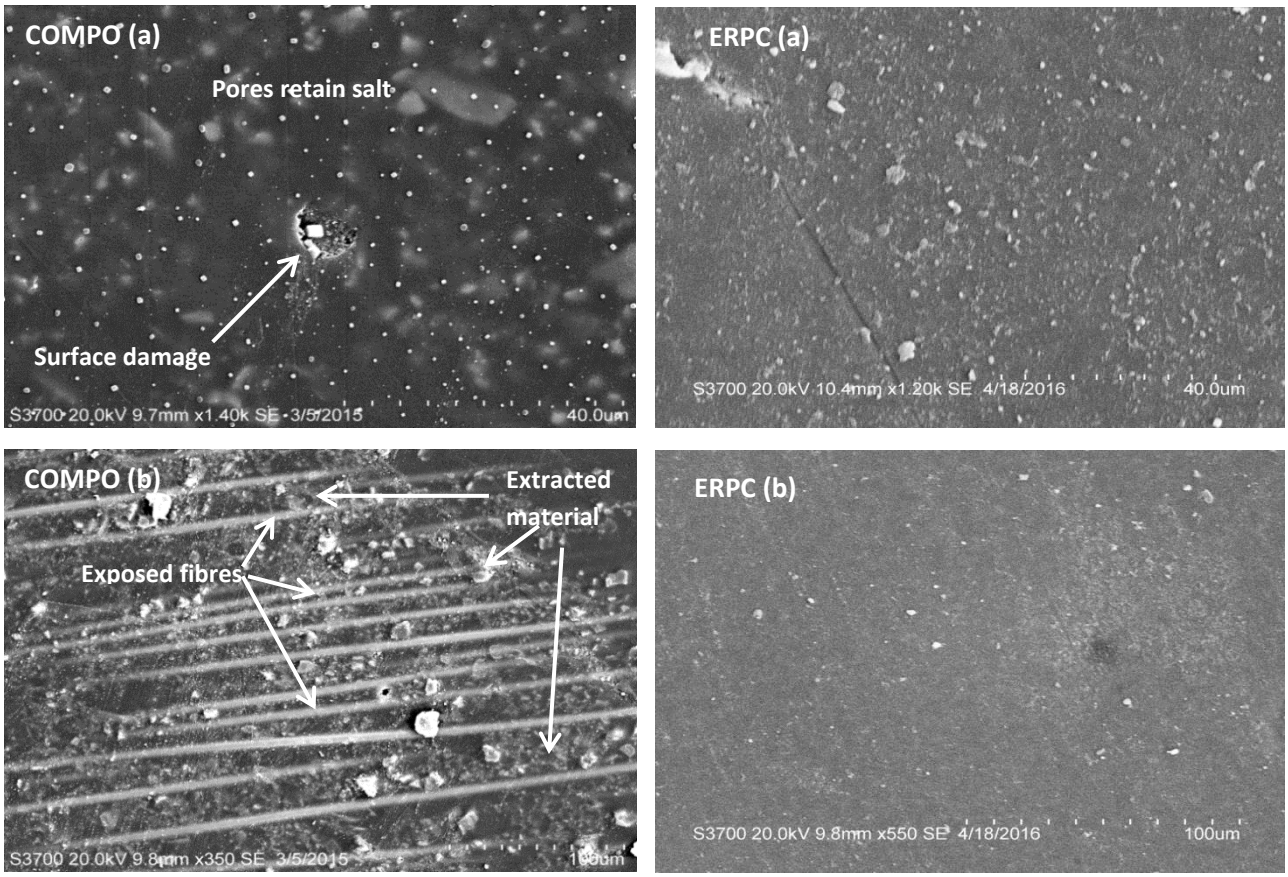

Fig. 6 – Exposed surfaces after a test in NaCl solution at 60^{o} angle of attack, composite: COMPO (a) site 1, COMPO (b) site 2; coatings: ERPC (a) site 1 and ERPC (b) site 2.

Figures 4, 5 show the SEM micrographs and EDX analysis of uncoated and coated specimens tested in NaCl solution at angle of attack 60^{o} respectively. Figure 4 COMPO(a, b) shows that the pores on the exposed uncoated surface have absorbed NaCl solution, which result in gain in mass after the test carried out. The retained NaCl, which seems to be dried on the exposed surface, is confirmed by EDX analysis Fig. 4COMPO(c, d). Figure 5 shows that there are no pores on the coated exposed surface and no NaCl has been retained by the coatings.

Figure 6 COMPO(a, b) shows the damage of the uncoated exposed surface, exposure of the reinforcement fibres and extruded material as a result of NaCl solution erosion. The presence of NaCl in water interacting with the composite exposed surface leads to de-bonding of the matrix and reinforcement along with erosion effects. Figure 6 ERPC (a, b) shows that the polymeric coatings protected the composite surface from NaCl solution erosion and there is no damage of the coated exposed surface as well. The coatings have protected the substrate surface from interaction and erosive effects of the NaCl solution.

Moreover, it has been proved that this polymeric coating is neither soluble nor is chemically reactive with seawater.

3.2. In NaCl Solution + Sand I and Sand II slurries

3.2.1. Volume loss of uncoated and coated composite in NaCl solution + Sand I (200 ± 50 µm), and Sand II (425 ± 175 µm) slurries.

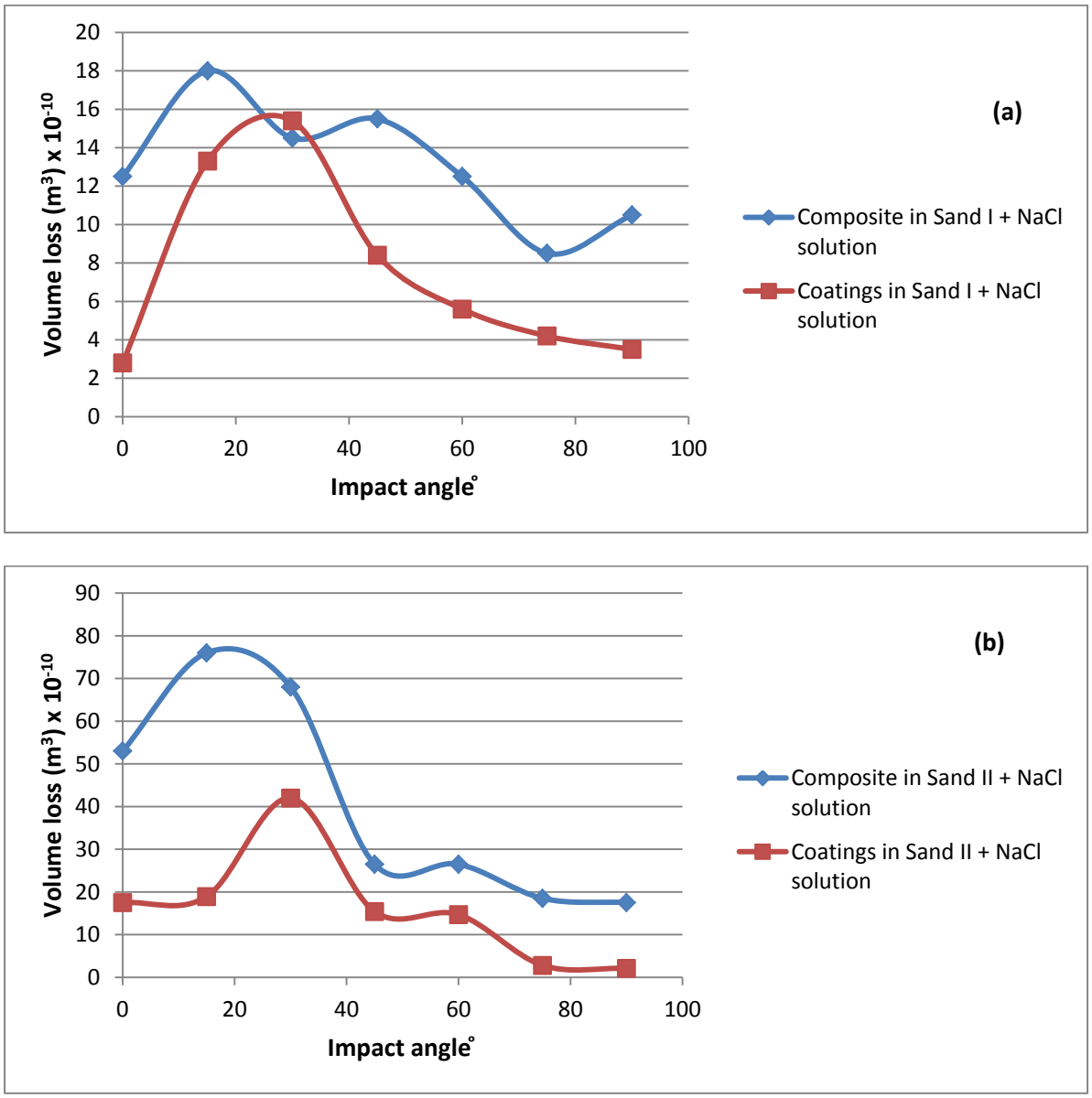

Fig. 7 – Volume loss comparison of composite and coatings specimens as a function of impact angle in NaCl solution (a) in Sand I + NaCl solution slurry (b) in Sand II + NaCl solution slurry.

Figures 7(a, b) show the volume loss comparison of composite, uncoated and coated with polymeric coatings specimens, in NaCl solution + S I and S II sand slurries respectively. In both slurries, maximum volume loss of composite occurred at impact angle 15°, while the maximum mass loss of polymeric coatings was occurred at impact angle 30°. Moreover, the composite is showing the uncertain erosive wear behaviour in different slurries, while the

coatings are showing similar erosive wear trends) in different slurries. The possible different erosive behaviour of uncoated and coated material may be attributed to their different mechanical properties, as the composites are anisotropic while polymeric coatings are isotropic materials. The fluctuation in erosive wear peaks can also be attributed to the different slurries, angles of attack, particles characteristics and material as composites behave differently than metals [14]. The uncoated material shows semi ductile erosive behaviour while the polymeric coating is showing quasi-ductile behaviour (maximum wear rate at 25 – 45° of attack). The erosive wear results of the polymeric coatings are in agreement with the Joseph Zahavi et al., solid particle erosion of polymeric coatings erosion tests results [15].

Furthermore, in both slurries, the minimum volume loss of the uncoated composite occurred at impact angle 75 – 90°, while in the case of coatings, the minimum volume loss occurred at all angles of attack except 30°, Fig.7. Therefore, due to application of coatings, the composite can be used for the extended range of angles of attack with minimum volume loss in such (marine) environment, which make composite a strong candidate (material) for tidal turbine blade application.

Figure 7(a, b) also reveals that the volume loss of the uncoated and coated composite has increased with an increase in particles size i.e. in Sand I (200 ± 50 µm), and Sand II (425 ± 175 µm) + NaCl solution. This is in agreement with research work in literature as the rate of erosion increases with the increase of particles size, hardness and angularity; however, at higher solid particle concentrations this increase cannot be prominent as the kinetic energy of the particles is dissipated partly due to the particle–particle collisions, to the blanketing effect, and to the decrease in particle rotation [5, 9, 16].

3.3. SEM micrographs of the exposed surfaces of uncoated and coated composite in NaCl solution + Sand I (200 ± 50 µm) slurry .

3.3.1. SEM micrographs of the exposed surfaces of uncoated and coated composite in NaCl solution + Sand I slurry at different impact angles.

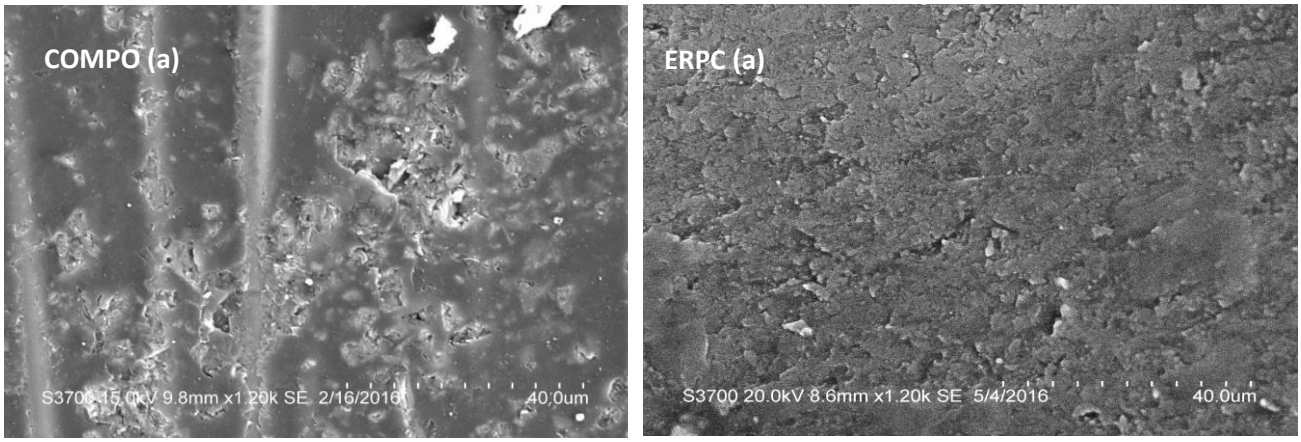

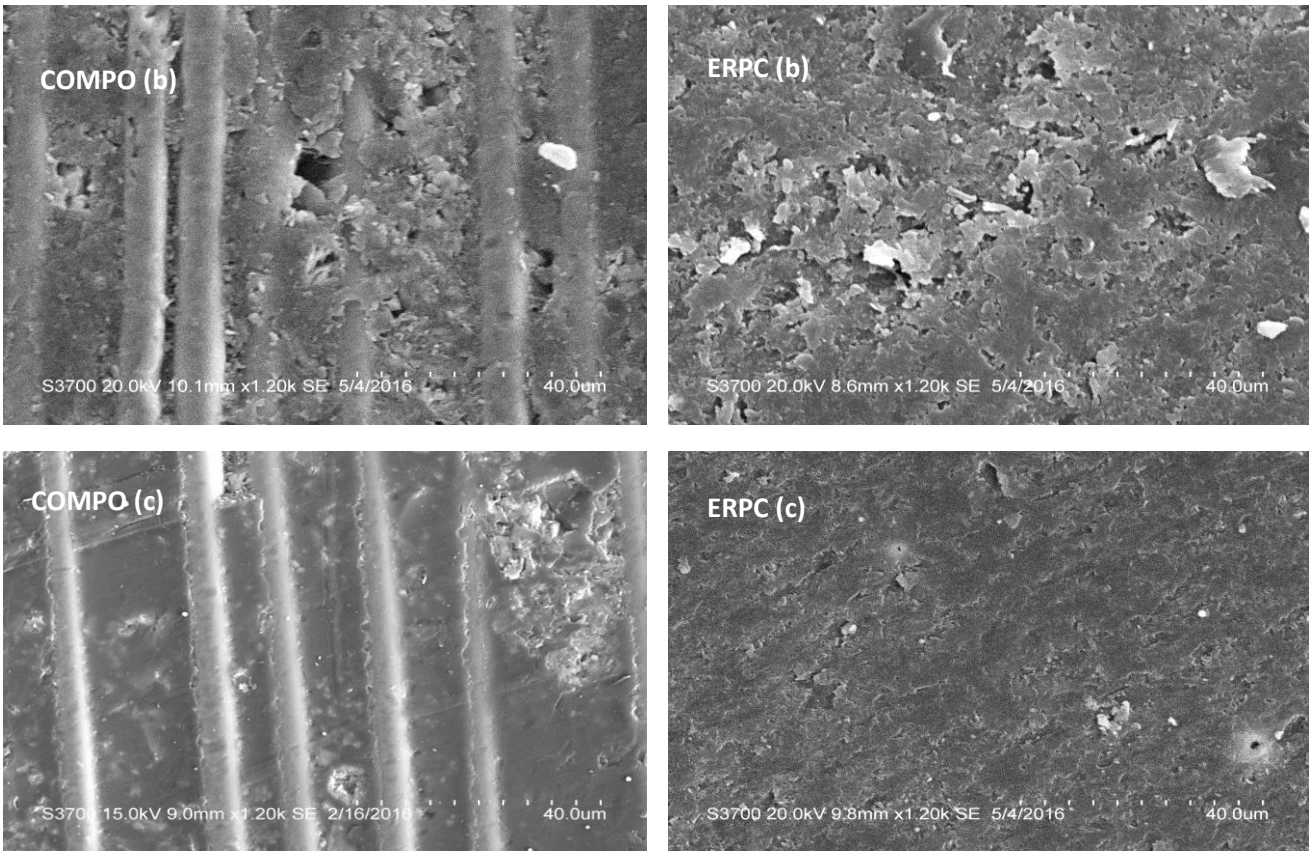

Fig. 8 – SEM micrographs of the exposed surfaces of composite and composite base polymeric coatings in NaCl solution + Sand I, (a) at impact angle 15°, (b) at impact angle 30°, and (c) at impact angle 60°.

3.3.2. SEM micrographs of the exposed surfaces of uncoated and coated composite in NaCl solution + Sand II (425 ± 175 µm) slurry at different impact angles.

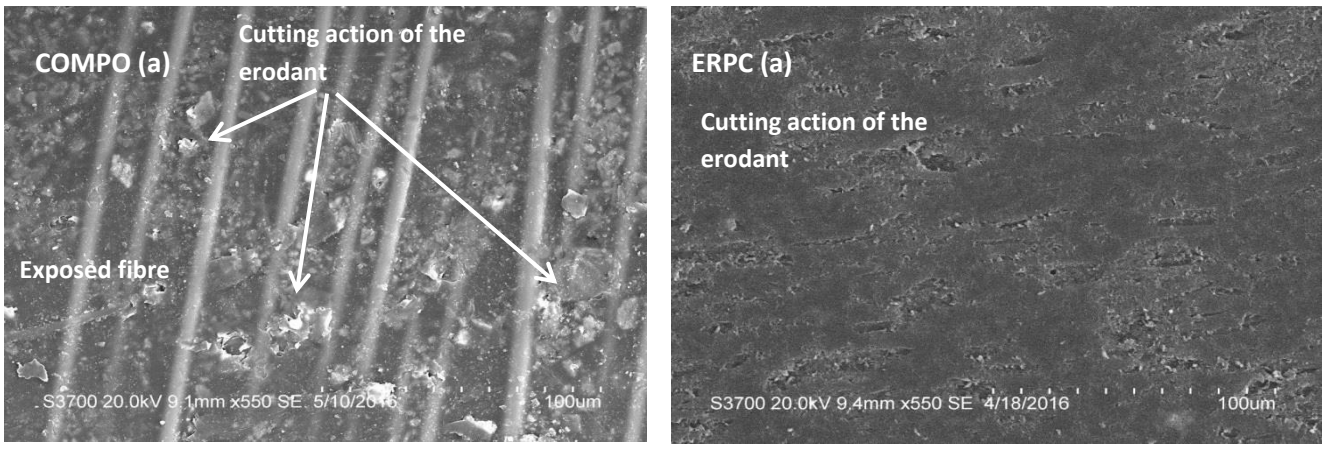

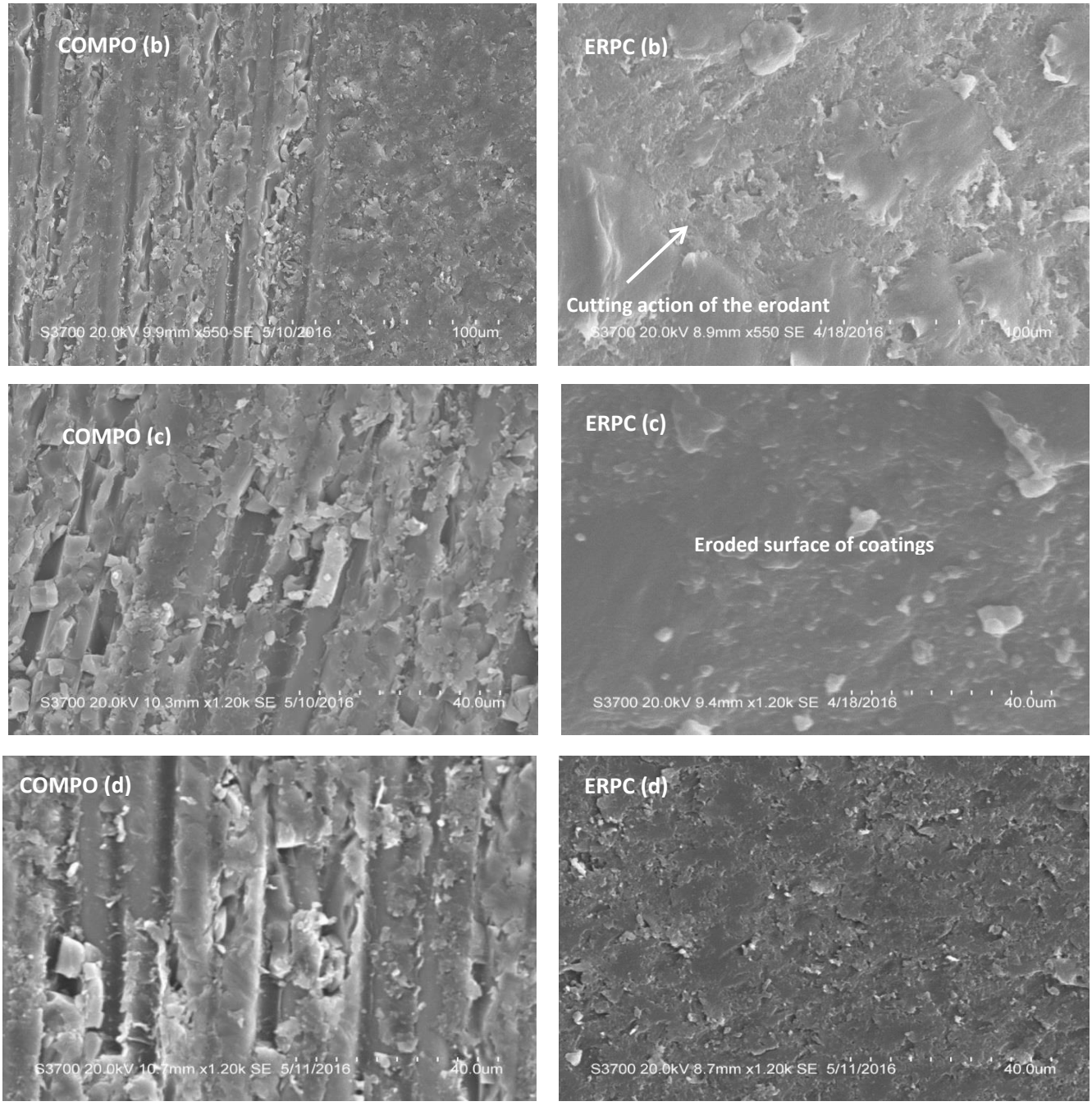

Fig. 9 – SEM micrographs of the exposed surfaces of composite and composite base polymeric coatings in NaCl solution + Sand II, (a) at impact angle 15^{o}, (b) at impact angle 30^{o}, (c) at impact angle 60^{o}, and (d) at impact angle 75^{o}.

Figures 8 - 9 show the morphologies of the eroded surfaces of uncoated and coated composite, coated with polymeric coatings, at different angles of attack and at constant blade tip speed in NaCl solution + Sand I and Sand II slurries. Both materials, composite and polymeric coatings, are showing different eroded surfaces morphologies, which, probably, are due to their different materials classes (categories). The effects of change in particles sizes are also apparent in these figures. For the composite, erosive wear becomes more

severe by the removal of material by cutting action and damages mechanisms by impact of erodent with an increase in solid particle size, Fig. 8 COMPO(a-c), 9 COMPO(a-d). For the coatings, erosive wear occurred by cutting action, which is peaking at 30^{o} angle of attack, Fig. 7 (a, b), 8 ERPC(a – c), and 9 ERPC(a – d). The surface roughness of the exposed surfaces of coatings seems to depend on mass loss, [15], while for uncoated, it depends on mass loss as well as on surface damages.

The cutting action of erodent is the predominant wear mechanism for both composite and coatings, in different slurries up to impact angle 30^{o}, Fig. 8-9 (a, b). For the other angles of attack, damage of exposed surfaces by impact of erodent is the predominant wear mechanism for uncoated materials [5], while there is no surfaces damage for coatings at these angles of attack, Fig. 8 (c), 9 (c, d), and the coating behaved in a ductile erosion manner. The most important factors affecting the erosion rate of materials are the impact velocity, impact angle of the erodent particles, the size, shape and hardness of the eroding particles, [9, 16, 17, 18]. The erosion mechanisms for both, uncoated and coated composites, appear similar. These observations are seem to be in agreement with the theory of erosion advanced by Bitter, which is based on the assumption that for an angle of attack <10°, erosion occurs due to chip formation at micro-scale, as a result of cutting action of erodent. For a 90° angle impact wear occurs, where during a 10–90° angle, both mechanisms contribute to the erosive wear [19].

Glass fibres mixtures at high cvolume fractions may act like a typical brittle material, so that erosion mainly occurrsby damage mechanisms as micro-cracking or plastic deformation due to the impact of solid particle. In brittle manner, damage is supposed to increase with the increase of kinetic energy loss [21]. According to Hutching et al. [22], kinetic energy loss is at a maximum at angles of impact of 90°, where erosion rates are maximum for brittle materials at similar impact angles (depending on the particle to target impact conditions). Erosion of polymers occurs in ductile manner, as stated above;, ductile materials have a peak erosion rate around 30° since the cutting mechanism dominates in erosion at such impact angles[21]. The erosion test results of the present work for composite (uncoated and coated with polymeric coatings) are in agreement of the above observations

Generally, it is thought that wear is based on loss of material, but it should be emphasized that damage due to material displacement or plastic deformation on a given body, damage of surface etc., without any change in weight or volume, is also called wear [20]. In view of the test results of this work and survey of the literature, the uncoated composite has very poor erosion resistance [21, 23]. In NaCl solution and NaCl solution + sand slurries, there are several tribological issues of the composite material Which need to be addressed in order to improve the performanceIt is also known that the erosive wear resistance of polymer composites is usually lower than that of the un-reinforced polymer matrix [24]. On the other hand, the composite base polymeric coating has increased the erosive wear resistance of this material with respect to above issues. In spite of higher volumes loss by erodent at 30^{o}

angle of attack in both slurries, Fig. 8-9 ERPC (c), the coatings not only protected substrate but also offer good adhesion, no evidence of cracking and damage through the substrate.

Experimental results reveal that due to the operational requirement of tidal turbine blade in erosive and contaminated environments, the erosion resistance of the polymeric composites may be of a high concern. The G10 epoxy glass laminate has presented a relatively unfavourable r erosion resistance despite having high stiffness and strength. However, its relative strength may be used to support an an erosion resistant polymeric coating, to make it suitable for tidal turbine blade applications.

4. Conclusions

1. Polymeric coatings exposed to simulated seawater slurry environments for tidal turbine simulation acted as barrier between uncoated composite and NaCl solutions.2. Uncoated composites showed evidence of erosive wear behaviour due to its material class i.e. anisotropic. . Polymeric coatings exhibited ductile erosive behaviourin such conditions.

3. The application of polymeric coatings increases the range of impact angles with minimum volume loss and exposed surface damages.

4. In the conditions tested, it was found that coatings increase the erosion resistance of the composite and did not wear through the substrate during erosion tests at different experimental conditions.

Acknowledgements

The authors would like to acknowledge the support of the EPSRC Supergen Grand Challenges Grant No EP/K013319/1, “Reducing the Costs of Marine Renewables via Advanced Structural Materials (ReC-ASM)” and thank The Advanced Materials Group in Newcastle University for providing the test samples and Belzona Polymerics Limited for coating test samples.

References

[1] http://www.smartgrids.eu/documents/New-ERA-for-Electricity-in-Europe.pdf.

[2] I. E. A. R. E. T. D. (IEA-RETD), Offshore Renewable Energy: Accelerating the Deployment of Offshore Wind, Tidal, and Wave Technologies. Routledge, 2011, p. 328.

[3] D. M. Grogan, S. B. Leen, C. R. Kennedy, and C. M. Ó Brádaigh, “Design of composite tidal turbine blades,” *Renew. Energy*, vol. 57, pp. 151–162, 2013.

[4] J. N. Goundar and M. R. Ahmed, “Design of a horizontal axis tidal current turbine,” *Appl. Energy*, vol. 111, pp. 161–174, Nov. 2013.

[5] Ghulam Rasool, Shayan Sharifi, Cameron Johnstone and Margaret M. Stack, Mapping synergy of erosion mechanisms of tidal turbine composite materials in sea water conditions, Bio-Tribo-Corrosion,

[6] A. Abouel-Kasem, Y. M. Abd-elrhman, K. M. Emara, and S. M. Ahmed, “Design and Performance of Slurry Erosion Tester,” *J. Tribol.*, vol. 132, no. 2, p. 021601, Apr. 2010.

[7] G. R. Desale, B. K. Gandhi, and S. C. Jain, “Improvement in the design of a pot tester to simulate erosion wear due to solid–liquid mixture,” *Wear*, vol. 259, no. 1–6, pp. 196–202, Jul. 2005.

[8] A. A. Gadhikar, A. Sharma, D. B. Goel, and C. P. Sharma, “Fabrication and Testing of Slurry Pot Erosion Tester,” *Trans. Indian Inst. Met.*, vol. 64, no. 4–5, pp. 493–500, Dec. 2011.

[9] W. Tsai, J. A. C. Humphrey, I. Cornet, and A. V. Levy, “Experimental measurement of accelerated erosion in a slurry pot tester,” *Wear*, vol. 68, no. 3, pp. 289–303, May 1981.

[10] James F. Newill, Steven H. McKnight, Cristopher P. R. Hoppel and Gene R. Cooper, Effects of Coatings on Moisture Absorption in Composite Materials, Army Research Laboratory, Weapon and Materials Research Directorate, ARL-2099, October 1999.

[11] G. Huang, Behaviours of glass fiber/unsaturated polyester composites under sea water environment, Mater. Des., 30 (2009), pp. 1337–1340

[12] David Mille, John F. Mandell, Daniel D. Samborsky, Bernadette A. Hernandez- Sanchez and D. Todd Griffith, Performance of Composite Materials Subjected to Salt Water Environments, 2012 AIAA SDM Wind Energy Session.

[13] Bin Wei, Hailin Cao and Shenhua, Degradation of basalt and glass fibre/epoxy resin composites in seawater, Corrosion Science, Vol. 53, January 2011, PP 426-431.

[14] B. D. Jana and M. M. Stack, A note on threshold velocity criteria for modelling the solid particle erosion of WC/Co MMCs, Wear, Vol. 270, no. 7-8, PP. 439-445, March 2011.

[15] J. Zahavi and G. F. Schmitt, “Solid particle erosion of reinforced composite materials,” *Wear*, vol. 71, no. 2, pp. 179–190, Sep. 1981.

[16] M. Lindgren and J. Perolainen, Slurry pot investigation of the influence of erodant characteristics on the erosion resistance of austenitic and duplex stainless steel grades, wear, Vol. 319, no. 1-2, PP. 38-48, Nov. 2014.

[17] Bhushan B., Principles and applications of Tribology, New York: Wiley; 1999.

[18] Joshua Salik and Donald H, Buckley, Effects of erodant particle shape and various heat treatments on erosion resistance of plain carbon steel, NASA Technical Paper 1755, Lewis Research Centre, Cleveland, Ohio.

[19] J.W.M. Mens and A.W.J. de Gee, Erosion in seawater slurries, Tribology International, Vol. 19, issue 2, PP. 59-64, April 1986.

[20] Bharat Bhushan, Introduction to Tribology, ISBN 0-471-15893-3, Page 331.

[21] Tamer Sinmazcelik, Isa Taskiran, Erosive wear behaviour of polyphenylenesulphide (PPS) composites, Materials and Design 28 (2007) 2471-2477.

[22] Hutching IM, Winter RE, Field JE., Solid particle erosion of metals: the removal of surface material by spherial projectiles, Proc Roy Soc Lond, Ser A 1976;348:379-392.

[23] Barkoula N-M, Karger-Kocsis J., Effects of fibre content and relative fibre orientation on the solid particle erosion of GF/PP composites, Wear 252, (2002), Pages 80-87.

[24] Hager A., Friedrich K., Dzenis Y. A., Paipetis S. A., Study of erosion wear of advanced polyemer composites, In: Street K. Whistler BC, editors, Proceedings of the ICCM-10, Canada. Cambridge: Woodhead Publishing Ltd.; 1995, Page 155-162.